An In Vitro Intestinal Model Captures Immunomodulatory Properties of the Microbiota in Inflammation

Jaclyn Y. Lock
Northeastern University
Mariaelena Caboni
Northeastern University
Philip Strandwitz
Northeastern University
Madeleine Morrissette
Northeastern University
Kevin DiBona
Northeastern University
Brian A. Joughin
Massachusetts Institute of Technology
Kim Lewis
Northeastern University
Rebecca L. Carrier (rebecca@coe.neu.edu)
Northeastern University https://orcid.org/0000-0003-3002-7098

Research

Keywords: Gut microbiome, Inflammation, Intestinal model, Gut simulator

Posted Date: October 9th, 2020

DOI: https://doi.org/10.21203/rs.3.rs-87438/v1

Abstract

Background

There is a growing appreciation for the significance of the gut microbiome in health and disease. Specifically, considerable effort has been put forth to understand mechanisms by which the microbiota modulates and responds to inflammation. Here, we explored whether oxidation metabolites produced by the host during inflammation, sodium nitrate and trimethylamine oxide, impact the composition of a human stool bacterial population in a gut simulator. We then assessed whether an immune-competent *in vitro* intestinal model responded differently to spent medium from bacteria exposed to these cues compared to spent medium from a control bacterial population.

Results

The host-derived oxidation products were found to decrease levels of *Bacteroidaceae* and overall microbiota metabolic potential, while increasing levels of pro-inflammatory *Enterobacteriaceae* and lipopolysaccharide in bacterial cultures, reflecting shifts that occur *in vivo* in inflammation. Spent medium, with or without sodium nitrate and trimethylamine oxide, induced elevated intracellular mucin levels and reduced intestinal monolayer integrity as reflected in trans-epithelial electrical resistance relative to fresh medium controls. However, multiplexed cytokine analysis revealed markedly different cytokine signatures from intestinal cultures exposed to spent medium with added oxidation products relative to spent control medium, while cytokine signatures of cultures exposed to fresh media were similar regardless of addition of host-derived cues. Further, the presence of immune cells in the intestinal model was required for this differentiation of cytokine signatures.

Conclusions

This study indicates that simple *in vitro* immune-competent intestinal models can capture bacterial-mammalian cross-talk in response to host-derived oxidation products and supports utility of these systems for mechanistic studies of interactions between the gut microbiome and host in inflammation.

Background

The human gastrointestinal tract harbors more than 10 trillion microbes [1], collectively known as the gut microbiota. This complex community has recently been linked to numerous components of human health and disease, including conditions related to metabolic, immune, and brain health [2]. Alterations to the microbiome due to infection, antibiotic treatment, a compromised immune system, or diet can result in microbial dysbiosis [3]. Inflammatory conditions of the intestinal tract, such as inflammatory bowel disease (IBD), have been associated with an increased abundance of facultative anaerobes belonging to the class of Gammaproteobacteria, mostly *Enterobacteriaceae*, over obligate anaerobes, such as *Bacteroides* and beneficial *Bifidobacteria* [4-11]. Oxidation products (e.g., nitrates, trimethylamine N-oxide (TMAO) and dimethyl sulfoxide) generated from host-derived antimicrobial radicals during intestinal

inflammation can be utilized by Gram-negative bacteria of the *Enterobacteriaceae* family as terminal electron acceptors for anaerobic respiration, allowing for their rapid growth and successful niche establishment in the gut [12, 13]. The lipopolysaccharide (LPS) of the *Enterobacteriaceae* outer membrane is a highly reactogenic microbe-associated molecular pattern (MAMP) that promotes the secretion of pro-inflammatory cytokines, nitric oxide, and eicosanoids by monocytes, dendritic cells, macrophages and B cells [7]. This cyclic process driven by the microbiome-host cross-talk can exacerbate intestinal inflammation [14].

The mucosal surface is the predominant site of interaction between the host and the gut microbiota and its derived metabolites, small molecule messengers, and MAMPs [15, 16]. The host epithelial layer produces a physical mucus barrier, which restricts bacterial penetration and molecule diffusion, and is composed of enterocytes, goblet cells, enteroendocrine cells, Paneth cells, and microfold cells [17]. An *in vitro* cell culture model consisting of an intestinal absorptive epithelial cell line (Caco-2) and a mucus-producing goblet cell line (HT29-MTX) has been frequently used to represent the intestinal epithelium, for example to investigate the permeability of drugs [18-20], or to measure microbial adhesion [21, 22]. Recently, dendritic cells representing immune cells in the gut have been added to the Caco-2/HT29-MTX cell culture system to obtain a more representative intestinal model [23, 24]. Within the intestine, dendritic cells are recruited to injury sites and can extend dendrites into the lumen to capture resident bacteria [25], therefore contributing to the microbiota-host communication locally and systemically.

Herein, we investigated whether 1) *in vitro* cultures of microbiota populations would be modified in response to inflammatory oxidation products (exogenous nitrate and TMAO), and 2) a simple *in vitro* intestinal model is capable of capturing immunomodulatory effects of molecules released by microbiota populations in response to these cues. A simple gut simulator fermentation system (Lewis Gut Simulator – LEGS [26]) was utilized to cultivate human gut microbiota communities in pro-inflammatory (exposure to sodium nitrate and TMAO) or control conditions. Filtered supernatant from these bacterial populations was then exposed to an immune-competent intestinal culture model of Caco-2/HT29-MTX/dendritic cells. Mucin production, monolayer integrity, and cytokine secretion were examined. Our results indicated modulation of microbiota structure and function *in vitro* in response to exposure to nitrate and TMAO mimicking the expansion of *Enterobacteriaceae* in conditions of intestinal inflammation. The shift in microbial population corresponded with reduced metabolic capacity and increased endotoxin levels, and bacterial-derived molecules in the spent media resulted in a distinct cytokine profile in the intestinal model. This simple *in vitro* immune-competent gut model reflects the exacerbated inflammatory response to dysbiosis in the gut, and thus could potentially be useful in screening therapeutic interventions.

Results

Human stool samples were inoculated in a simplified human gut simulator (LEGS) in regular (GIFU) or pro-inflammatory (pGIFU; containing nitrate and TMAO) microbial media, and cultures were analyzed by 16S rRNA V4 amplicon sequencing for microbial composition analysis. After a week of culture, microbiota communities comprising more than 20 bacterial families were maintained in the two different

culture conditions. The composition of the microbial population in pGIFU was severely altered as compared to the control GIFU culture (Fig 1A, Supplement A). For the most abundant families with a relative abundance greater than 10%, we observed a 2.2-fold increase in *Enterobacteriaceae* and a 1.5-fold decrease in *Bacteroidaceae* in pGIFU. Among bacteria present at an intermediate abundance of 1-10%, *Methanobacteriaceae* and several microbial families of the Firmicutes phylum (i.e. *Ruminococcaceae*, *Lachnospiraceae, Veillonellaceae*) were reduced in pGIFU. On the contrary, *Clostridiaceae*, Proteobacteria members of the *Desulfovibrionaceae* family, and Bacteroidetes of the *Porphyromonadaceae* family were increased in pGIFU pro-inflammatory culture. Although possessing a similar species richness index in the alpha-diversity analysis (Supplemental Fig 1), the pGIFU microbial community was characterized by a significant decrease in the overall genomic potential as compared to GIFU microbiota, especially in key metabolic functions, including metabolism of amino acids, carbohydrate, lipid, and vitamins, and general energy metabolism, as shown in the metagenomic KEGG pathway abundance analysis by PICRUSt (Fig 1B, Supplement A).

In order to isolate molecules released by the microbiota communities, culture supernatants were filtered to remove bacterial cells and obtain spent media, GIFU-S and pGIFU-S. Pro-inflammatory pGIFU-S had significantly higher endotoxin levels compared with GIFU-S (Fig 1C). We then tested whether microbiota-derived molecules in spent media from the different gut simulators were able to differentially modulate homeostasis of intestinal culture models. Both “epithelial only” cultures (i.e. Caco-2/HT29-MTX co-culture, -DC) and “immune-competent” cultures (i.e. Caco-2/HT29-MTX/DC co-culture, +DC) were tested. There was no significant difference in the number of epithelial cells after 24 hr exposure to fresh or spent media, as shown by total DNA quantification (Fig 2A), indicating that the presence of microbial byproducts did not induce extensive cell death or proliferation. The incorporation of DCs on the basolateral side of the Transwell® membrane did not significantly impact monolayer integrity (i.e. % change in TEER from day 0 were similar) when compared to cultures without DCs. However, in +DC cultures, a marked and significant reduction in TEER due to exposure to spent (GIFU-S and pGIFU-S) vs. fresh (GIFU and pGIFU) media was observed, while TEER of -DC cultures was only reduced moderately after exposure to GIFU-S relative to GIFU (Fig 2B). TEER values of all cultures exposed to spent media were lower than those of control cultures exposed to serum-free intestinal medium, with this difference more pronounced in +DC cultures. Interestingly, pro-inflammatory nitrate and TMAO factors in fresh media or their reduced derivatives from microbial anaerobic respiration in spent media did not significantly impact TEER values, as seen in comparisons of cultures exposed to GIFU vs. pGIFU based-media. To directly observe changes to the monolayer, we stained for cell tight junctions, which regulate epithelial paracellular permeability [27], and we measured production of mucin, a major constituent of the intestinal mucosal barrier [28]. In monolayers exposed to control serum-free intestinal medium and GIFU, ZO-1 tight junction staining appeared as a continuous belt-like structure (Fig 3). Monolayers exposed to GIFU-S and pGIFU had a zig-zag ZO-1 staining pattern, while pGIFU-S-exposed monolayers had areas of low staining, suggesting spent microbial media and supplementation with nitrate/TMAO impacted monolayer integrity [29, 30].

Exposure to fresh and spent microbial media affected the amount of intracellular and extracellular mucin. We observed a statistically significant increase in intracellular mucin in monolayers cultured with DCs and exposed to spent media compared to fresh media, i.e. GIFU vs GIFU-S and pGIFU vs pGIFU-S (Fig 4A). In addition, all test media, including fresh GIFU and pGIFU, increased intracellular mucin in immune-competent cultures relative to control serum-free intestinal medium. In contrast, in cultures -DC, the impact of spent vs. fresh media on mucin was only statistically significant in cultures containing inflammatory factors, i.e. pGIFU vs pGIFU-S, and was less marked than for immune-competent cultures. Levels of secreted mucin had greater variability but were generally higher in test media relative to control serum-free intestinal medium (Fig 4B).

To assess whether the bacterial products in spent media, and, in particular, bacterial products in media containing pro-inflammatory factors, resulted in a measurable and specific immune response, apically secreted levels of 27 cytokines were quantified after exposure of intestinal monolayers to test media. Pairwise hierarchical clustering, performed to explore correlations of cytokine response among samples, revealed that cytokine secretion signatures were similar within each treatment, as media groups generally clustered together (Fig 5). The fresh media, GIFU and pGIFU, generally clustered together, as did spent media groups GIFU-S and pGIFU-S. The incorporation of dendritic cells resulted in a different cytokine signature compared to epithelial-only cultures exposed to the same media. For most of the cytokines analyzed, the secreted levels were similar in overall magnitude between epithelial-only and immune-competent models, with the exception of IL4 and GM-CSF, which were higher in cultures +DC (Supplemental Fig 2). However, responses to bacterial factors in spent media relative to fresh media were generally more distinct in immune-competent models.

Unsupervised PCA analysis revealed that two orthogonal linear combinations of cytokine levels, PC1 and PC2, captured 81.8% of the covariance in the dataset for cultures +DC (Fig 6A) and 70.1% for cultures -DC (Fig 6B). In cultures -DC, PC1 accounted for 54.2% of the variability, discriminating serum-free intestinal vs. microbial media, while PC2 accounted for 15.9% of the variability, discriminating fresh vs. spent bacterial media. In cultures +DC, PC1 accounted for 70.1% of the variability, discriminating fresh vs. spent media, while PC2 accounted for 11.7% of the variability, discriminating different types of fresh medium (serum-free intestinal control vs. GIFU-based media). Interestingly, a distinct response to spent bacterial media with and without the pro-inflammatory cues (pGIFU-s vs. GIFU-S), but not corresponding fresh media (pGIFU vs. GIFU), was reflected in PC1 and PC2 for immune-competent cultures, while cytokine profiles of cultures -DC did not reflect a distinct response to shifted bacterial factors resulting from exposure to pro-inflammatory cues (pGIFU-S vs GIFU-S).

The PCA loadings plot depicts the relative contribution of each cytokine to PC1 and PC2 (Fig 6C, D). In epithelial-only cultures, loadings on PC1 were positive for all cytokines, reflecting generally elevated levels in fresh and spent GIFU-based media relative to serum-free intestinal medium control. In immune-competent cultures, loadings on PC1 were positive for most cytokines, reflecting overall increase in inflammatory cytokine levels in cultures exposed to spent media relative to fresh media. However, exposure to fresh nutrient-rich GIFU media but not media that was spent by bacteria or serum-free

intestinal medium control markedly elevated a small subset of immune mediators (IP10, MIP1b, and RANTES) as reflected in their negative and positive loadings on PC1 and PC2 in immune-competent and epithelial-only cultures, respectively (Fig 5, Supplemental Fig 2, Fig 6C, D), suggesting a potential response to nutritional cues.

Many measured cytokines showed a pattern of elevation in response to spent bacterial media relative to fresh medium in immune-competent cultures, as reflected in positive loading on PC1 (Supplemental Fig 2, Fig 6C), but did not show a differential response to pro-inflammatory cues (i.e. pGIFU-S vs. GIFU-S). IL6 response was most distinctly impacted by bacterial factors in spent media in immune-competent cultures, while levels in epithelial-only cultures were higher when exposed to fresh nutrient-rich bacterial media than in spent media and control, suggesting a differential response to nutritional or bacterial factors depending on the presence of immune cells in the model. GM-CSF levels were markedly higher in +DC relative to -DC cultures and significantly increased upon exposure of +DC cultures to spent media over fresh media. A similar pattern of response to bacterial factors in +DC cultures was observed for PDGF, although only significant in comparison to control (i.e. pGIFU-S and GIFU-S vs. control). Other cytokines reflected a clear response to bacterial factors in immune-competent cultures, but at lower measured apical levels (< 10 pg/ml, Supplemental Fig 2), such as TNFα and IFNγ. Still other cytokines were at low apical levels and showed a more moderate response to bacterial factors, including IL1β, Eotaxin, and IL7.

A cytokine subset showed a pattern of elevation in response to bacterial factors in pro-inflammatory spent GIFU medium relative to regular spent GIFU medium in immune-competent cultures. Signals of IL8, IL12, and VEGF were statistically significantly increased in pGIFU vs. GIFU spent medium, with this difference evident only in cultures +DC, as reflected in loadings on PC2 (Fig 6C, Supplemental Fig 2). In contrast, some cytokines significant in maintenance of intestinal homeostasis (IL10, IL4) were notably more elevated in cultures +DC exposed to bacterial factors resulting from regular medium (GIFU-S vs. GIFU) than pro-inflammatory medium (pGIFU-S vs. pGIFU). IL1ra, IL2, G-CSF, IL17 and FGFb levels showed a similar pattern, evident in both immune-competent and epithelial-only cultures.

Discussion

A simplified gut simulator (LEGS) simulated shifts in the human gut microbiome when exposed to host-derived inflammatory cues. The increase in *Enterobacteriaceae* in pGIFU cultures supplemented with nitrate and TMAO (Fig 1A) mimics the *Enterobacteriaceae* bloom observed in the inflamed gut previously studied in different *in vivo* animal models of colitis [12, 13], as well as in patients with ulcerative colitis and Crohn's disease [5]. The decrease in several families in the Firmicutes phylum and the increase in Proteobacteria in pGIFU cultures reflect a microbial signature reported in gnotobiotic mice with active colitis relative to those in remission [31]. Specifically, Proteobacteria (*Enterobacteriaceae* and *Desulfovibrio*) were associated with colitis, and Actinobacteria, Firmicutes and Bacteroidetes with anti-inflammatory remission conditions [31]. The alteration in microbial composition was accompanied by a shift in population functionality. We observed an increase in pro-inflammatory LPS endotoxin (reflecting

the increased abundance in *Enterobacteriaceae*) [7], and a change in microbial metabolic potential, with pGIFU microbiota being associated with a reduced capacity for energy harvest, similar to previous reports of studies in active *in vivo* colitis models [31].

Microbial molecules and metabolites have been shown to influence cell proliferation, intestinal permeability and immune signaling both *in vitro* and *in vivo* [32, 33]. After 24 hr exposure to either fresh or spent microbial media, there was no impact on epithelial cell number (Fig 2A), which is consistent with previous work that showed that 24 hr exposure to 10 μg/ml LPS did not significantly affect cell number of Caco-2 cultures [34]. However, TEER was significantly impacted by exposure to spent media, with a pronounced effect observed in immune-competent cultures, reflecting the important role immune cells play in sensing bacterial molecules. The decrease in TEER may be attributed to the increase in endotoxin levels in spent media compared to fresh media (Fig 2B), and may reflect a partial disruption of tight junctions, supported by imaging of ZO-1 (Fig 3), which has previously been implicated in the development of leaky gut in intestinal diseases [27].

Within the gastrointestinal tract, extracellular mucin binds microbes preventing their penetration into the epithelium [35-37]. Mucin synthesis and secretion can be activated by microbial products, toxins, and cytokines [38]. For example, LPS from *Helicobacter pylori* and *Escherichia coli* alter mucin gene expression and secretion in human goblet cell lines and in rodent models [39]. Although the fresh media do not contain any microbial products or toxins, the rich nutritional content of the bacterial medium may have impacted mucin production, in particular in +DC cultures (Fig 4). The addition of dietary fibers (i.e. 0.5g/L soluble starch in GIFU media) has been previously shown to increase goblet cell volume in the small intestine [40]. Dietary fibers can also be digested by members of the microbiota resulting in the synthesis of short-chain fatty acids, which have also been shown to increase MUC2 mRNA levels in goblet-like LS174T cells [41], and may have contributed to the observed increase in intracellular mucin levels in cultures exposed to spent media.

The analysis of the intestinal model cytokine response suggested activation of signaling pathways that are relevant to host-microbial interactions [42]. Detected cytokine levels in epithelial cultures -DC reflect the fact that not only immune cells, but also the intestinal epithelium is in itself an important producer of cytokines [43]. Reports of production of cytokines by the epithelium, and significance of cytokines specifically to intestinal inflammation, are noted in the discussion below. The overall similar absolute cytokine levels in epithelial-only and immune-competent models (Supplemental Fig 2) likely is due in part to the measurement of apical cytokines, mostly influenced by epithelia present at the apical interface. Similarly, co-culture of primary small intestinal epithelium with macrophages was not reported to change apical levels of IL8, IFNγ or IL6, while basolateral levels increased markedly with the presence of macrophages [44]. Indeed, the levels of apical factors analyzed in this study likely better reflect values of intestinal lumen contents, but might vary significantly from basolateral secretion levels for some cytokines [44-46]. The incorporation of immune cells did distinctly alter cytokine profiles after exposure to fresh or spent microbial media (Fig 5, Fig 6, Supplemental Fig 2). It is possible that some reported cytokine levels reflect both basolateral secretions from DCs and apical factors modulated by the

epithelial-immune crosstalk, given the ability of DCs to infiltrate the epithelium [47], and the increased permeability, reflected in TEER, of cultures exposed to bacterial factors.

Most of the cytokines assessed in the multiplex panel showed a general pattern of elevation upon exposure to bacterial factors in spent as compared to fresh media, especially in immune-competent cultures (i.e. significant differences between both GIFU-S and pGIFU-S with respective fresh media were observed for IL6, GM-CSF, TNFα, INFγ, Eotaxin, and IL10 in +DC cultures) (Fig 5, Fig 6C-D, and Supplemental Fig 2). Notable exceptions include elevation in fresh vs. spent media of IP10, MIP1β, and RANTES in both +DC and -DC cultures, IL6 and IL7 in -DC cultures, and IL1ra and G-CSF in pGIFU-based media (Fig 5, Fig 6C-D, and Supplemental Fig 2). This may indicate a response to nutritional cues which are depleted in spent media due to microbial metabolism.

Cytokines elevated in spent vs. fresh media have known roles in response to bacterial factors and intestinal inflammation. IL6, a pleiotropic cytokine central in regulating inflammatory responses, is released by both immune (e.g., monocytes and macrophages), and epithelial cells [48], and is important in attracting inflammatory cells and activating T and B lymphocytes. Together with other inflammatory cytokines such as TNFα and IFNγ, elevation of IL6 has been demonstrated to negatively affect the intestinal epithelial barrier function [43], in agreement with what we observed in immune-competent cultures exposed to spent media (Fig 2B). TNFα, a central immune cytokine produced by dendritic cells, stimulates T-cells to produce IFNγ [49]. TNFα□□production by intestinal epithelial cells has been implicated in intestinal inflammation, with most significant secretion likely occurring basolaterally to impact underlying mesenchymal cells [50]. IFNγ is produced mainly by T lymphocytes and NK cells, but production by epithelial cells and DCs has been reported [51]. GM-CSF has been demonstrated to be produced by colon epithelium and plays an important role in impacting intestinal epithelial proliferation in response to injury [52] as well as recruitment of DCs in response to pathogen invasion [53]. Eotaxin is important in allergic response, is significantly produced by the intestinal epithelium [54], and its role in intestinal inflammation is increasingly recognized [55, 56]. IL10 is an anti-inflammatory cytokine produced primarily by Treg cells in the gut [57].

Factors elevated in response to fresh vs. spent media, potentially due to nutritional cues present in fresh media, also are important in intestinal immune function. IP10, MIP1b, and RANTES are produced by intestinal epithelia as well as immune cells and have been implicated in inflammatory, metabolic or diet-related conditions [58-61]. The shift of IL6 and IL7 from being elevated in fresh media in epithelial-only cultures to being elevated in spent media in +DC cultures reflects the significance of immune cells in the mucosal model's response to bacterial factors. Intestinal epithelial cells also produce IL7 [62], which can impact IL4 production by immune cells.

The differential response to spent vs. fresh pGIFU and GIFU media observed for levels of IL1ra and G-CSF could signify suppression of these cytokines by factors present in the pro-inflammatory bacterial cultures. IL1ra has been demonstrated to be produced at elevated levels at the apical surface of cervical epithelium [63], and at biologically relevant (with respect to modulating IL1β) levels by oral mucosal

epithelium [64]. IL1ra plays the important role of inhibiting the effect of pro-inflammatory IL1β by binding to its receptor, and its modulation by microbial factors has been associated with reduced intestinal inflammation and tissue damage [65, 66]. G-CSF plays a role in maintenance of homeostasis [67] and is important in promoting survival of recruited polymorphonuclear cells in the intestine. It has been used as an efficacious therapy in some patients with Crohn's disease [68]. G-CSF was shown to be produced by airway epithelium in response to bacterial stimulation [69].

The incorporation of immune cells in our intestinal model was not only required for bacterial stimuli to be the major discriminating factor in cytokine signature, but was also key for inducing a differential cytokine signature to pro-inflammatory microbiota versus control microbiota, as reflected in separation of pGIFU-S and GIFU-S on the principal component scores plot (Fig 5, Fig 6, Supplemental Fig 2). Indeed, in immune-competent cultures, the change in bacterial factors in response to pro-inflammatory cues (pGIFU-S vs GIFU-S) resulted in significant elevation of IL8, IL12 and VEGF (reflected in positive loadings on principal components 1 and 2 on the scores plot, Fig 6A). IL8 is produced by multiple cell types including monocytes and epithelial cells and regulates host response to microbial factors by acting as a chemoattractant for neutrophils. It has been demonstrated that bacteria differentially modulate production of IL8 by epithelial cells [70]. Polarized (apical) secretion of IL8 by intestinal epithelium has been demonstrated to be stimulated by ligand binding to Toll-like receptor 2 (TLR2) and TLR5 [46, 71], which are major receptors for MAMPs including LPS, lipoproteins and flagellin [72]. IL12 has been reported to be produced mainly by monocytes in the intestine, but airway epithelium has been demonstrated to produce IL12 in inflammation [73], and elevation of this Th1-inducing factor has been observed in intestinal inflammatory conditions in humans and animal models [74]. VEGF is a key mediator of angiogenesis, a process highly integrated with inflammation, is produced by intestinal epithelial cells in response to microbial stimuli, and impacts epithelial as well as vascular biology [75, 76].

In contrast to cytokines elevated in response to pro-inflammatory bacterial factors (pGIFU-S vs. pGIFU), there were several cytokines that showed the opposite trend. Induction of cytokines by bacterial factors in pro-inflammatory media (i.e. level in pGIFU-s/level in pGIFU) was relatively lower than induction in regular bacterial media (i.e. level in GIFU-S/level in GIFU) for IL10, IL4, IL17, and FGFb (Fig 5, Fig 6C, Supplemental Fig 2), as well as IL1ra and G-CSF, which were discussed above in light of decrease in pGIFU-S vs. pGIFU. IL10 has been long recognized as a key mediator of intestinal immune regulation by the microbiota [77, 78]. IL4 has anti-inflammatory and inflammatory actions depending on context, and is able to promote release of IL10, as well as TGFβ regulatory cytokines [79]. IL4 is the most potent polarizing cytokine for Th2 differentiation, primarily produced by Th2 cells in the gut and by a subset of monocyte-derived inflammatory DCs [80]. Thus, elevated IL4 in DC-containing cultures could be a result of production by DCs, or, as the DCs were derived from human leukocytes and likely do not represent a pure population, by other leukocyte populations. IL4 expression in Caco-2 and HT29 cell lines has also been previously reported [81]. IL4 is a potent inhibitor of IL8 [82], which may in part explain elevated levels of IL8 in immune-competent gut models exposed to pGIFU-S relative to GIFU-S. IL17, which is produced by both immune and non-immune cells, was relatively low in expression level, but is central in governing a protective immune response at mucosal sites and regulating interactions with the microbiota. FGFb has

been demonstrated to be secreted at significant levels, which are elevated in inflammatory bowel disease, at the apical intestinal mucosal surface [83].

Overall, several cytokines suppressed by pGIFU-S relative to GIFU-S, including IL1ra and G-CSF discussed above, have known roles in inhibiting inflammatory cytokines and/or maintenance of homeostasis. Combined with elevation of inflammatory cytokines (IL8, IL12, VEGF), the specific cytokine signature observed upon exposure to pGIFU-S media suggest that molecules produced by the microbiota in response to inflammatory conditions (nitrate and TMAO), reflecting altered microbial composition and associated elevated endotoxin levels, produce a dominant and distinct pro-inflammatory response which may disrupt the immunological equilibrium. On the contrary, increased levels of some cytokines, such as IL10, in models exposed to regular GIFU-S may reflect cellular measure to counteract excessive monolayer-damaging inflammation and could be induced by regulatory microbial molecules or other medium components to restore homeostasis [57].

It is noted that cytokines actively trigger signaling in the 5-100 pM range. Many of the values reported are below or at the lower end of this range. Other recent reports from primary intestinal cells (as opposed to intestinal cell lines employed here) showed higher levels of some cytokines [44, 71], including apical IL8 and MCP1, being more than an order of magnitude greater than what was measured here. These disparities might reflect differences between primary and cell line cultures, and in culture conditions (culture area, media type and volume, time of sampling). However, levels of IL8 [46, 82] and MCP1 [84] previously measured in Caco-2 cultures, as well as of VEGF in T84 cell line [75] were comparable to those measured here. IFNγ and IL6 amounts secreted in apical media of primary colonic epithelium were similar to those reported here for Caco-2/HT29 cultures [44]. Also, low levels of some inflammatory cytokines may reflect their primary production *in vivo* by cells not present in the intestinal cultures employed in these studies. Finally, our model can be considered to approximate the function of the colon, as both Caco-2 and HT29 are derived from colonic tissue, and the microbial consortia were derived from stool. However, primary cultures derived from a specific part of intestine (e.g., jejunum or colon) could be used to more precisely model region-specific intestinal functions.

The varied response of cytokines observed in this study reveals an intricate modulation of host-microbiota cross-talk. It is noted that only multiplex cytokine analysis capturing a broad range of secreted factors, paired with PCA and hierarchical analyses, clearly differentiated the variable response to bacterial factors reflecting a shift to an altered bacterial population induced by proinflammatory factors, while all other analyses described above (i.e. monolayer integrity, ZO-1 staining, mucin production) reflected a marked response only to spent vs fresh media. Further, if select factors had been analyzed (e.g., TNFα and IL6) as opposed to a broad array of cytokines and chemokines, the differential response to the proinflammatory culture may not have been evident.

Conclusions

Microbial communities prepared in a simple gut simulator (LEGS) can be utilized in combination with human intestinal cultures to study immune-mediated cross-talk between the microbiota and the host. The supplementation of host-derived metabolites produced during inflammation (nitrate and TMAO) resulted in a bloom of pro-inflammatory *Enterobacteriaceae* which was accompanied by elevated endotoxin levels and reduced metabolic potential, compared to microbial communities cultured in regular GIFU media. Caco-2/HT29-MTX/dendritic cell monolayer integrity, as well as the production of mucin were altered upon exposure to spent medium from bacterial cultures, but these metrics did not differentiate response to regular GIFU-S relative to inflammatory pGIFU-S media. Multiplex cytokine analysis, however, revealed distinct cytokine signatures differentiating the response to fresh versus spent media, and importantly the response to spent pro-inflammatory vs. control bacterial GIFU media. The incorporation of dendritic cells in the intestinal culture model was required for differential response to the pro-inflammatory (pGIFU-S) vs control spent bacterial (GIFU-S) medium as reflected in PCA. Finally, PCA revealed a subset of elevated cytokines (i.e. upregulated IL8, IL12, VEGF; and downregulated IL1ra) reflecting an exacerbated inflammatory response to metabolites and molecules generated by the pro-inflammatory microbiota as compared to the control microbial community. These results highlight the utility of a simple immune-competent *in vitro* intestinal models paired with multiplex cytokine analysis as a useful tool in recapitulating and providing insight into the microbial and immune signatures observed in intestinal inflammation. Such models can be explored for in-depth analysis of microbiome-gut-immune cross-talk, as well as to screen potential therapeutic interventions.

Methods

Lewis Gut Simulator (LEGS) and Microbiota Spent Media

Microbiota communities from human stool were grown in a 1:10 dilution of rich GIFU anaerobic medium (HiMedia®) [85] composed of 10 g/L peptone, 3 g/L soya peptone, 10 g/L protease peptone, 13.5 g/L digested serum, 5 g/L yeast extract, 2.2 g/L meat extract, 1.2 g/L liver extract, 3 g/L dextrose, 2.5 g/L potassium dihydrogen phosphate, 3 g/L sodium chloride, 5 g/L soluble starch, 0.3 g/L L-cysteine hydrochloride, and 0.3 g/L sodium thioglycolate, maintained at pH 7 by the addition of 50 mM 3-(N-morpholino)propanesulfonic acid (MOPS, ThermoFisher Scientific) buffer. Pro-inflammatory GIFU (pGIFU) was composed of GIFU anaerobic media supplemented with 4mM sodium nitrate (Sigma Aldrich) and 4 mM TMAO (Sigma Aldrich).

A LEGS gut simulator was used to culture human gut communities in either GIFU or pGIFU media under anaerobic conditions (vinyl anaerobic chamber, Coy Laboratory Products, Inc.). The system was built and operated as previously described [26], with some modifications. A bottle of sterile de-oxygenated medium was attached to a sequential two-chamber chemostat. Sterile silicon tubing (3/32” ID x 5/32” OD) connected the media vessel to the first chamber, which was connected to the second chamber via additional 3/32” ID x 5/32” OD tubing and peristaltic tubing (size 0.89mm). 1 ml aliquots of a stool sample diluted 10^5 in deoxygenated medium were inoculated into both chambers on the first day of the

experiment, and then media was pumped into the first chamber so that the entire volume (150 mL) was replaced every 24 hrs. The system is designed such that components of the fresh medium are utilized by the microbial community, and the breakdown products of metabolism are then transitioned to the second chamber (akin to what happens in the human GI tract) at the same rate fresh media is pumped into the first chamber. For the present experiment, a single LEGS system was prepared with each medium (GIFU and pGIFU), and after one week of culture, samples of the LEGS communities were collected from the second chamber for V4 16S rRNA amplicon sequencing. In parallel, the microbial community from the second chamber was pelleted by centrifugation, and spent medium was 0.22 µm filtered to remove live and dead bacteria, and stored at -80 °C prior to use in *in vitro* culture models. These samples will be referred to as GIFU-S and pGIFU-S for spent regular and pro-inflammatory GIFU media, respectively.

16S rRNA Amplicon Sequencing and Microbiota Dataset Analysis

DNA extraction and sequencing were performed by Mr. DNA (Shallowater, TX, USA) with a Roche 454 FLX. Amplification of the V4 variable region was performed using PCR primers 515F/806R in a 30 cycle PCR with the HotStarTaq Plus Master Mix Kit (Qiagen, USA). The following conditions were used: 94˚C for 3 minutes and 30 cycles of 94˚C for 30 seconds, 53˚C for 40 seconds and 72˚C for 1 minute, followed by a final elongation step at 72˚C for 5 minutes. Data were demultiplexed and quality filtered in and analyzed using Quantitative Insights into Microbial Ecology (QIIME™) [86]. Operational taxonomic unit (OTU) and feature tables were generated, respectively, in QIIME1 using a closed-reference protocol based on the Greengenes database [87] and in QIIME2 [88] using the vsearch dereplicate-sequences command. Taxonomy was assigned to the feature table using the Greengenes 13-8 classifier, and the family level relative abundance is reported. The functional contents of the metagenome were predicted using PICRUSt [89] using default parameters based on the closed-reference OTU table. Identified gene families (KEGG Orthology groups) were grouped into metabolic pathways based on the BRITE hierarchy, and relative abundance of clustered Level 3 pathways was compared (Supplement A).

Quantification of Endotoxin Levels in Microbiota Spent Media

Endotoxin concentration in fresh and spent media was quantified using Pierce Limulus Amebocyte Lysate Chromogenic Endotoxin Quantification Kit (ThermoFisher Scientific). Briefly, a microplate was equilibrated on a heating block for 10 mins at 37 °C. 50 µl of each test medium (GIFU, pGIFU, GIFU-S, or pGIFU-S) or standard was added to a separate well, followed by addition of 50 µl of Limulus Amebocyte Lysate solution and incubation for 10 min at 37 °C. The chromogenic substrate solution (100 µl) was added to each well and incubated for 6 mins at 37 °C. Finally, 50 µl of the stop reagent (25% acetic acid) was added, and the absorbance was measured at 405 nm using a BioTek Powerwave XS

spectrophotometer. The standard curve ranged from 0-1.0 endotoxin units (EU)/ml and was used to calculate the concentration of the samples that were run in triplicate.

In Vitro Cell Culture Model

Human intestinal carcinoma epithelial (Caco-2 clone C2BBe1, ATCC) and mucus-producing (HT29-MTX-E12, Sigma Aldrich) cells were cultured in Advanced Dulbecco's Modified Eagle's Medium (DMEM, ThermoFisher Scientific) supplemented with 10% heat-inactivated fetal bovine serum (Atlanta Biologics), 1x GlutaMax™ (ThermoFisher Scientific), and 1x Penicillin/Streptomycin (P/S, ThermoFisher Scientific). Caco-2 (passage 55-65) and HT29-MTX (passage 35-45) cells were seeded in 9:1 ratio on 24 well Transwell® inserts (Falcon™) at a density of 10^5 cells/cm^2. Briefly, the apical and basal sides of the Transwell® membrane were coated with 50 µg/ml collagen type I from rat tail (Corning®) in phosphate buffered saline (PBS, ThermoFisher Scientific) for 2 hrs at room temperature. Caco-2 and HT29-MTX were harvested from culture flasks using 0.25% Trypsin-EDTA (ThermoFisher Scientific) to obtain single cells for seeding onto the apical side of the Transwell® membrane. Culture medium was replaced every 2 days (apical: 300 µl, basolateral: 700 µl). One week post-seeding, the medium was changed to serum-free intestinal medium composed of Advanced DMEM, 1x GlutaMax™, 1x P/S, 1x Insulin-Transferrin-Sodium Selenite (Roche Diagnostics).

Dendritic cells (DCs) derived from human blood monocytes were incorporated as the immune component of the co-culture model [23, 24]. Briefly, peripheral blood mononuclear cells were isolated from Human Peripheral Blood Leuko Pak (STEMCELL™ Technologies) using EasySep™ Human Monocyte Enrichment Kit (STEMCELL™ Technologies). Monocytes were differentiated into dendritic cells using Advanced RPMI medium (Gibco) supplemented with 1x GlutaMax™, 1% P/S, 50 ng/ml granulocyte/macrophage colony-stimulating factor (GM-CSF, Biolegend®), 35 ng/ml interleukin 4 (Biolegend®), and 10 nM retinoic acid (Sigma Aldrich). After 7 days of differentiation, dendritic cells were harvested using accutase™ (STEMCELL™ Technologies) and seeded on the basolateral side of the Transwell® membrane used to culture Caco-2/HT29-MTX for 2 weeks as described above, at a 1:10 ratio of dendritic cells:epithelial cells. Briefly, apical medium was removed, and the Transwell® was gently inverted. 75 µl dendritic cell suspension was added to the membrane and incubated for 30 mins at 37 °C and 5% CO_2, after which the Transwell® was gently placed back into the 24 well culture plate. Caco-2/HT29-MTX cultures in Transwell® inserts with and without dendritic cells were maintained for an additional week in serum-free media. Medium was changed every other day.

Exposure of Intestinal Cells to Microbiota Spent Media

Cells in the *in vitro* model were exposed to microbiota spent (GIFU-S or pGIFU-S) or fresh (GIFU or pGIFU) GIFU-based media, or serum-free intestinal cell culture media as control. Apical and basolateral chambers

were washed with 500 µl of PBS prior to exposure to test media. PBS in the apical chamber was removed and replaced with 300 µl of test medium, PBS in the basolateral chamber was removed and replaced with 700 µl serum-free intestinal medium, and the cultures were incubated for 24 hrs at standard cell culture conditions (37 °C and 5% CO_2).

Trans-epithelial electrical resistance (TEER) measurements were made prior to exposure to test media and after 24 hr exposure. An EndOhm-24SNAP chamber with an EVOM2 meter (World Precision Instruments) was used to measure TEER. Samples and media were kept warm at 37 °C prior to measurement to minimize variability between TEER measurements due to temperature fluctuations. Percent change from the original TEER measurement was calculated.

After 24 hr exposure, apical and basolateral media samples were collected and stored at -80 °C. Caco-2 and HT29-MTX cells were lysed to analyze intracellular mucin concentration. Briefly, apical and basolateral chambers were each washed with 500 µl PBS. After removing PBS from both chambers, cells were placed overnight at -80 °C. The plate was then thawed on ice for 10 mins and 500 µl lysis buffer (50 mM Tris(hydroxymethyl)aminomethane, 10% glycerol, 150 mM sodium chloride, 1% NP-40, all chemicals from Sigma Aldrich) was added to each apical compartment. The Transwell® membrane surface was then scraped with a pipet tip to remove all cells, and scraped material was collected in a microcentrifuge tube. Each sample was vortexed for 1 min and placed on ice for 30 mins on a shaker. A mini bead beater mill (Cole-Parmer®) was used to homogenize the sample for 20 secs. Samples were centrifuged at 10,000 g for 10 mins at 4 °C to remove cellular debris, and the supernatant was analyzed for mucin and DNA concentration.

Mucin Quantification

Secreted and intracellular mucin concentrations were quantified using the alcian blue assay [90]. Briefly, 100 µl of sample was loaded into a 96 well plate and 33.4 µl of alcian blue (Sigma Aldrich) was added. The plate was equilibrated on a shaker for 2 hrs at room temperature and then centrifuged for 30 mins at 1870 xg. The plate was washed twice with 100 µl of wash buffer (40% ethanol, 0.1 M sodium acetate, 25 mM magnesium chloride, at pH 5.8, all chemicals from Sigma Aldrich). The pellet was then resuspended in 100 µl of 10% sodium dodecyl sulfate (Sigma Aldrich). Sample absorbance was measured at 620 nm using a BioTek Powerwave XS spectrophotometer. A standard solution of 0-250 µg/ml mucin from bovine submaxillary glands (Sigma Aldrich) was used to quantify the concentration of unknown samples.

DNA Quantification

CyQUANT® cell proliferation assay kit (ThermoFisher Scientific) was used to measure DNA concentration. Briefly, the lysed cell supernatant was supplemented with 1 mM ethylenediaminetetraacetic acid (EDTA, Sigma Aldrich) to prevent DNA degradation. In a 96 well plate, 100 µl of standards, samples, or blank and 100 µl of CyQUANT® GR dye was added and incubated for 5 mins at room temperature. The fluorescence

of the samples (480/520 $\lambda_{ex}/\lambda_{em}$) was measured using EnSight™ multimode plate reader (PerkinElmer, Inc.). Bacteriophage λ DNA was used to make a standard curve ranging from 0-1000 ng/ml.

Caco-2/HT29-MTX Monolayer Staining for ZO-1

After exposure to test media, apical and basolateral chambers were washed with 500 µl PBS, fixed with 500 µl 4% paraformaldehyde (Sigma Aldrich) in PBS overnight at 4 ºC, washed with 1x PBS, and permeabilized with 0.4% Triton-X (Sigma Aldrich) in PBS for 30 mins at room temperature. To minimize non-specific interactions, apical and basolateral chambers were blocked with 2.5% goat serum (500 µl, Sigma Aldrich) in PBS for 30 mins at room temperature. The tight junction protein zonula occluden (ZO-1) was stained with Alexa Fluor 488 conjugated ZO-1 monoclonal antibody (5 µg/ml, apical chamber only, ThermoFisher Scientific) overnight at 4 ºC. Cell nuclei were stained with 4', 6-Diamidino-2-Phenylindole, Dihydrochloride (DAPI, 300 nM, apical chamber only, ThermoFisher Scientific) for 30 mins at room temperature. Images of the stained monolayer were obtained using Zeiss Axio Observer Z1 with attached X-Cite® 120LED and Hamamatsu ORCA-Flash 4.0 Digital Camera.

Multiplex Cytokine Assay

Cytokine levels were measured using Bio-Plex Pro™ Human Cytokine 27-plex Assay (Bio-Rad Laboratories, Inc.). To minimize non-specific binding of proteins to antibody-coupled magnetic beads, bovine serum albumin (BSA) was added to each sample to achieve a final concentration of 5 mg/ml. The protein standard was diluted in serum-free medium supplemented with BSA. The assay was run according to manufacturer protocol. Briefly, 50 µl beads were added to each well, and each well was then washed 2x with 100 µl Bio-Plex wash buffer using Bio-Plex Pro™ Wash Station. Next, 50 µl of samples, standards, or blank was added to each well and incubated on a shaker at 850 rpm for 1 hr at room temperature. The wells were washed 3x with 100 µl wash buffer, 1x detection antibody was added, and the plate was incubated on a shaker at 850 rpm for 1 hr at room temperature. The wells were again washed 3x with 100 µl wash buffer, 50 µl Streptavidin, R-Phycoerythrin Conjugate (SA-PE) was added, and the plate was incubated on a shaker at 850 rpm for 10 mins at room temperature. After a final 3x wash with 100 µl wash buffer, the beads were resuspended in 125 µl of assay buffer and incubated on a shaker at 850 rpm for 30 sec. The plate was analyzed using a Bio-Plex™ 200 System and Bio-Plex™ Manager 6.1. The concentration of each cytokine was determined from the standard curve, which was generated by fitting a 5-parameter logistic regression of mean fluorescence on known cytokine concentrations. Samples were diluted to ensure the measurements were within the linear dynamic range of the assay.

Multivariate Analysis

Cytokine level data were normalized by mean-centering and unit scaling variance prior to hierarchical clustering and principal component analysis (PCA). Hierarchical clustering was completed using the

clustergram function in MATLAB® software (R2017B, Mathworks, Inc.). Mean centering is the subtraction of the mean from each individual value. Unit variance scaling is dividing the mean-centered data by the standard deviation of the mean-centered data. PCA was completed using MATLAB® software with the *pca* function. In PCA, the linear combination of cytokines that explains the highest possible amount of variance in the data is iteratively identified, and then removed from the data, converting the original cytokine data into linearly uncorrelated variables, called principal components (PC).

Statistical Analysis

All data are generally presented as a mean with standard deviation (STDEV). ANOVA and Tukey-Kramer post hoc test were used to determine significance with $\alpha = 0.05$. PICRUSt data in Fig 1B are presented as mean +/- standard error of the mean (SEM), and the Wilcoxon matched-pairs signed rank test was used to assess significance with $p < 0.05$.

Declarations

Ethics approval and consent to participate

The collection of human stool samples from healthy volunteers was approved by Northeastern University IRB# 08-11-16.

Consent for publication

Not applicable.

Availability of data and material

All data generated or analyzed during this study are included in this published article and its supplementary information files.

Competing interests

The authors declare that they have no competing interests

Funding

The authors acknowledge funding sources: March of Dimes (MoD #6-FY14-404), National Institutes of Health: National Institute of Biomedical Imaging and Bioengineering (R01-EB021908), National Institutes of Health: National Cancer Institute (NC1 U01-CA215798) for supporting Brian Joughin, US Army Natick Research Center (G00004945, Developing an Artificial Gut with a Diverse Microbiome), Northeastern University Dissertation Completion Fellowship, and U.S. National Science Foundation Graduate Research Fellowship Program for supporting Jaclyn Lock (GRFP 2012125281). Funding bodies did not participate in the design of the study and collection, analysis, and interpretation of data and in writing the

manuscript. The content is solely the responsibility of the authors and does not necessarily represent the official views of the National Institutes of Health.

Authors' contributions

MC and PS built and ran the LEGS system and conducted microbiome analysis. JL and KD cultured and analyzed the intestinal-immune model. MM aided in microbiota composition and genomic potential analysis. RC, KL, and all authors contributed to study conceptualization, data analysis and interpretation, as well as writing and editing the manuscript.

Acknowledgements

The authors thank Abigail Koppes for access to Zeiss microscope.

References

[1] Sender R, Fuchs S, Milo R. Revised Estimates for the Number of Human and Bacteria Cells in the Body. PLoS Biology 2016;14(8):e1002533.

[2] Knight R, Callewaert C, Marotz C, Hyde ER, Debelius JW, McDonald D, et al. The Microbiome and Human Biology. Annu Rev Genom Hum Genet 2017;18:65-86.

[3] Buttó LF, Haller D. Dysbiosis in intestinal inflammation: Cause or consequence. International Journal of Medical Microbiology 2016;306(5):302-9.

[4] Singh RK, Chang H-W, Yan D, Lee KM, Ucmak D, Wong K, et al. Influence of diet on the gut microbiome and implications for human health. Journal of translational medicine 2017;15(1):73.

[5] Swidsinski A, Ladhoff A, Pernthaler A, Swidsinski S, Loening-Baucke V, Ortner M, et al. Mucosal flora in inflammatory bowel disease. Gastroenterology 2002;122(1):44-54.

[6] Rosenfeld Y, Shai Y. Lipopolysaccharide (Endotoxin)-host defense antibacterial peptides interactions: Role in bacterial resistance and prevention of sepsis. BBA - Biomembranes 2006;1758(9):1513-22.

[7] Park BS, Lee J-O. Recognition of lipopolysaccharide pattern by TLR4 complexes. Experimental & Molecular Medicine 2013;45(12):e66.

[8] Kaur N, Chen C-C, Luther J, Kao JY. Intestinal dysbiosis in inflammatory bowel disease. 2011;2(4):211-6.

[9] Seksik P, Rigottier-Gois L, Gramet G, Sutren M, Pochart P, Marteau P, et al. Alterations of the dominant faecal bacterial groups in patients with Crohn's disease of the colon. Gut 2003;52(2):237-42.

[10] Frank DN, St. Amand AL, Feldman RA, Boedeker EC, Harpaz N, Pace NR. Molecular-phylogenetic characterization of microbial community imbalances in human inflammatory bowel diseases. Proceedings of the National Academy of Sciences of the United States 2007;104(34):13780-5.

[11] Baumgart M, Dogan B, Rishniw M, Weitzman G, Bosworth B, Yantiss R, et al. Culture independent analysis of ileal mucosa reveals a selective increase in invasive Escherichia coli of novel phylogeny relative to depletion of Clostridiales in Crohn's disease involving the ileum. The ISME Journal 2007;1(5):403-18.

[12] Winter SE, Winter MG, Xavier MN, Thiennimitr P, Pooh V, Keestra AM, et al. Host-derived nitrate boosts growth of E. coli in the inflamed gut. Science 2013;339(6120):708.

[13] Winter SE, Lopez CA, Bäumler AJ. The dynamics of gut-associated microbial communities during inflammation. EMBO reports 2013;14(4):319-27.

[14] Heimesaat MM, Fischer A, Siegmund B, Kupz A, Niebergall J, Fuchs D, et al. Shift Towards Pro-inflammatory Intestinal Bacteria Aggravates Acute Murine Colitis via Toll-like Receptors 2 and 4 (TLRs and Gut Flora in Colitis). PLoS ONE 2007;2(7):e662.

[15] Lavelle A, Sokol H. Gut microbiota-derived metabolites as key actors in inflammatory bowel disease. Nat Rev Gastroenterol Hepatol 2020;17(4):223-37.

[16] Grigg JB, Sonnenberg GF. Host-Microbiota Interactions Shape Local and Systemic Inflammatory Diseases. J Immunol 2017;198(2):564-71.

[17] Allaire JM, Crowley SM, Law HT, Chang SY, Ko HJ, Vallance BA. The Intestinal Epithelium: Central Coordinator of Mucosal Immunity. Trends Immunol 2018;39(9):677-96.

[18] Wikman-Larhed A, Artursson P. Co-cultures of human intestinal goblet (HT29-H) and absorptive (Caco-2) cells for studies of drug and peptide absorption. European Journal of Pharmaceutical Sciences 1995;3(3):171-83.

[19] Chen Y, Lin Y, Davis K, Wang Q, Rnjak-Kovacina J, Li CM, et al. Robust bioengineered 3D functional human intestinal epithelium. Sci Rep 2015;5.

[20] Pan F, Han L, Zhang Y, Yu Y, Liu J. Optimization of Caco-2 and HT29 co-culture in vitro cell models for permeability studies. International Journal Of Food Sciences And Nutrition 2015;66(6):680-5.

[21] Gagnon M, Zihler Berner A, Chervet N, Chassard C, Lacroix C. Comparison of the Caco-2, HT-29 and the mucus-secreting HT29-MTX intestinal cell models to investigate Salmonella adhesion and invasion. Journal of Microbiological Methods 2013;94(3):274-9.

[22] Laparra JM, Sanz Y. Comparison of in vitro models to study bacterial adhesion to the intestinal epithelium. Letters in Applied Microbiology 2009;49(6):695-701.

[23] Chen WLK, Edington C, Suter E, Yu J, Velazquez JJ, Velazquez JG, et al. Integrated gut/liver microphysiological systems elucidates inflammatory inter-tissue crosstalk. Biotechnology and Bioengineering 2017;114(11):2648-59.

[24] Tsamandouras N, Chen W, Edington C, Stokes C, Griffith L, Cirit M. Integrated gut and liver microphysiological systems for quantitative in vitro pharmacokinetic studies. An Official Journal of the American Association of Pharmaceutical Scientists 2017;19(5):1499-512.

[25] Rescigno M, Urbano M, Valzasina B, Francolini M, Rotta G, Bonasio R, et al. Dendritic cells express tight junction proteins and penetrate gut epithelial monolayers to sample bacteria. Nature Immunology 2001;2(4):361-7.

[26] O'Connor K, Morrissette M, Strandwitz P, Ghiglieri M, Caboni M, Liu H, et al. Cranberry extracts promote growth of Bacteroidaceae and decrease abundance of Enterobacteriaceae in a human gut simulator model. PLoS One 2019;14(11):e0224836.

[27] Lee SH. Intestinal permeability regulation by tight junction: implication on inflammatory bowel diseases. Intestinal research 2015;13(1):11-8.

[28] Larsson JM, Karlsson H, Sjovall H, Hansson GC. A complex, but uniform O-glycosylation of the human MUC2 mucin from colonic biopsies analyzed by nanoLC/MSn. Glycobiology 2009;19(7):756-66.

[29] Tang Y, Banan A, Forsyth CB, Fields JZ, Lau CK, Zhang LJ, et al. Effect of alcohol on miR-212 expression in intestinal epithelial cells and its potential role in alcoholic liver disease. Alcohol Clin Exp Res 2008;32(2):355-64.

[30] Lynn KS, Peterson RJ, Koval M. Ruffles and spikes: Control of tight junction morphology and permeability by claudins. Biochim Biophys Acta Biomembr 2020;1862(9):183339.

[31] Rooks MG, Veiga P, Wardwell-Scott LH, Tickle T, Segata N, Michaud M, et al. Gut microbiome composition and function in experimental colitis during active disease and treatment-induced remission. The ISME Journal 2014;8(7):1403.

[32] Ohland CL, Jobin C. Microbial Activities and Intestinal Homeostasis: A Delicate Balance Between Health and Disease. Cellular and Molecular Gastroenterology and Hepatology 2015;1(1):28-40.

[33] Postler TS, Ghosh S. Understanding the Holobiont: How Microbial Metabolites Affect Human Health and Shape the Immune System. Cell Metabolism 2017;26(1):110-30.

[34] Lin T-Y, Fan C-W, Maa M-C, Leu T-H. Lipopolysaccharide-promoted proliferation of Caco-2 cells is mediated by c-Src induction and ERK activation. BioMedicine 2015;5(1):1-6.

[35] Dekker J, Van Beurden-Lamers WM, Oprins A, Strous GJ. Isolation and structural analysis of rat gastric mucus glycoprotein suggests a homogeneous protein backbone. The Biochemical journal

1989;260(3):717-23.

[36] Johansson MEV, Phillipson M, Petersson J, Velcich A, Holm L, Hansson GC. The inner of the two Muc2 mucin-dependent mucus layers in colon is devoid of bacteria. PNAS 2008;105(39):15064-9.

[37] Larsson J, Karlsson H, Sjovall H, Hansson G. A complex, but uniform O-glycosylation of the human MUC2 mucin from colonic biopsies analyzed by nanoLC/MSn. Glycobiology 2009;19(12):1568-9.

[38] Andrianifahanana M, Moniaux N, Batra SK. Regulation of mucin expression: mechanistic aspects and implications for cancer and inflammatory diseases. Biochimica et biophysica acta 2006;1765(2):189-222.

[39] Cornick S, Tawiah A, Chadee K. Roles and regulation of the mucus barrier in the gut. Tissue Barriers 2015;3(1-2).

[40] Lundin E, Zhang JX, Huang CB, Reuterving CO, Hallmans G, Nygren C, et al. Oat Bran, Rye Bran, and Soybean Hull Increase Goblet Cell Volume Density in the Small Intestine of the Golden Hamster a Histochemical and Stereologic Light-Microscopic Study. Scandinavian Journal of Gastroenterology 1993;28(1):15-22.

[41] Burger-van Paassen N, Vincent A, Puiman PJ, van der Sluis M, Bouma J, Boehm G, et al. The regulation of intestinal mucin MUC2 expression by short-chain fatty acids: implications for epithelial protection. Biochemical Journal 2009;420:211-9.

[42] Kinnebrew MA, Pamer EG. Innate immune signaling in defense against intestinal microbes. Immunol Rev 2012;245:113-31.

[43] Onyiah JC, Colgan SP. Cytokine responses and epithelial function in the intestinal mucosa. Cell Mol Life Sci 2016;73(22):4203-12.

[44] Noel G, Baetz NW, Staab JF, Donowitz M, Kovbasnjuk O, Pasetti MF, et al. A primary human macrophage-enteroid co-culture model to investigate mucosal gut physiology and host-pathogen interactions. Sci Rep 2017;7:45270.

[45] Kominsky DJ, Campbell EL, Ehrentraut SF, Wilson KE, Kelly CJ, Glover LE, et al. IFN-gamma-mediated induction of an apical IL-10 receptor on polarized intestinal epithelia. J Immunol 2014;192(3):1267-76.

[46] Rossi O, Karczewski J, Stolte EH, Brummer RJ, van Nieuwenhoven MA, Meijerink M, et al. Vectorial secretion of interleukin-8 mediates autocrine signalling in intestinal epithelial cells via apically located CXCR1. BMC Res Notes 2013;6:431.

[47] Rescigno M, Urbano M, Valzasina B, Francolini M, Rotta G, Bonasio R, et al. Dendritic cells express tight junction proteins and penetrate gut epithelial monolayers to sample bacteria. Nat Immunol

2001;2(4):361-7.

[48] Krueger J, Ray A, Tamm I, Sehgal PB. Expression and function of interleukin-6 in epithelial cells. J Cell Biochem 1991;45(4):327-34.

[49] Beaurepaire C, Smyth D, McKay DM. Interferon-gamma regulation of intestinal epithelial permeability. J Interferon Cytokine Res 2009;29(3):133-44.

[50] Roulis M, Armaka M, Manoloukos M, Apostolaki M, Kollias G. Intestinal epithelial cells as producers but not targets of chronic TNF suffice to cause murine Crohn-like pathology. Proc Natl Acad Sci U S A 2011;108(13):5396-401.

[51] Resende M, Cardoso MS, Ribeiro AR, Florido M, Borges M, Castro AG, et al. Innate IFN-gamma-Producing Cells Developing in the Absence of IL-2 Receptor Common gamma-Chain. J Immunol 2017;199(4):1429-39.

[52] Egea L, McAllister CS, Lakhdari O, Minev I, Shenouda S, Kagnoff MF. GM-CSF produced by nonhematopoietic cells is required for early epithelial cell proliferation and repair of injured colonic mucosa. J Immunol 2013;190(4):1702-13.

[53] Hirata Y, Egea L, Dann SM, Eckmann L, Kagnoff MF. GM-CSF-facilitated dendritic cell recruitment and survival govern the intestinal mucosal response to a mouse enteric bacterial pathogen. Cell Host Microbe 2010;7(2):151-63.

[54] Kim E, Lembert M, Fallata GM, Rowe JC, Martin TL, Satoskar AR, et al. Intestinal Epithelial Cells Regulate Gut Eotaxin Responses and Severity of Allergy. Front Immunol 2018;9:1692.

[55] Adar T, Shteingart S, Ben Ya'acov A, Bar-Gil Shitrit A, Goldin E. From airway inflammation to inflammatory bowel disease: eotaxin-1, a key regulator of intestinal inflammation. Clin Immunol 2014;153(1):199-208.

[56] Adar T, Shteingart S, Ben-Ya'acov A, Shitrit AB, Livovsky DM, Shmorak S, et al. The Importance of Intestinal Eotaxin-1 in Inflammatory Bowel Disease: New Insights and Possible Therapeutic Implications. Dig Dis Sci 2016;61(7):1915-24.

[57] D'Hennezel E, Abubucker S, Murphy LO, Cullen TW. Total Lipopolysaccharide from the Human Gut Microbiome Silences Toll-Like Receptor Signaling. mSystems 2017;2(6): e00046-17.

[58] Kulkarni N, Pathak M, Lal G. Role of chemokine receptors and intestinal epithelial cells in the mucosal inflammation and tolerance. J Leukoc Biol 2017;101(2):377-94.

[59] Bondar C, Araya RE, Guzman L, Rua EC, Chopita N, Chirdo FG. Role of CXCR3/CXCL10 axis in immune cell recruitment into the small intestine in celiac disease. PLoS One 2014;9(2):e89068.

[60] Chang TT, Chen JW. Emerging role of chemokine CC motif ligand 4 related mechanisms in diabetes mellitus and cardiovascular disease: friends or foes? Cardiovasc Diabetol 2016;15(1):117.

[61] Chou SY, Ajoy R, Changou CA, Hsieh YT, Wang YK, Hoffer B. CCL5/RANTES contributes to hypothalamic insulin signaling for systemic insulin responsiveness through CCR5. Sci Rep 2016;6:37659.

[62] Jiang Y, McGee DW. Regulation of human lymphocyte IL-4 secretion by intestinal epithelial cell-derived interleukin-7 and transforming growth factor-beta. Clin Immunol Immunopathol 1998;88(3):287-96.

[63] Buckner LR, Lewis ME, Greene SJ, Foster TP, Quayle AJ. Chlamydia trachomatis infection results in a modest pro-inflammatory cytokine response and a decrease in T cell chemokine secretion in human polarized endocervical epithelial cells. Cytokine 2013;63(2):151-65.

[64] Perrier S, Kherratia B, Deschaumes C, Ughetto S, Kemeny JL, Baudet-Pommel M, et al. IL-1ra and IL-1 production in human oral mucosal epithelial cells in culture: differential modulation by TGF-beta1 and IL-4. Clin Exp Immunol 2002;127(1):53-9.

[65] Carvalho FA, Aitken JD, Gewirtz AT, Vijay-Kumar M. TLR5 activation induces secretory interleukin-1 receptor antagonist (sIL-1Ra) and reduces inflammasome-associated tissue damage. Mucosal Immunol 2011;4(1):102-11.

[66] Rogier R, Ederveen THA, Boekhorst J, Wopereis H, Scher JU, Manasson J, et al. Aberrant intestinal microbiota due to IL-1 receptor antagonist deficiency promotes IL-17- and TLR4-dependent arthritis. Microbiome 2017;5(1):63.

[67] Martins A, Han J, Kim SO. The multifaceted effects of granulocyte colony-stimulating factor in immunomodulation and potential roles in intestinal immune homeostasis. IUBMB Life 2010;62(8):611-7.

[68] Mannon PJ, Leon F, Fuss IJ, Walter BA, Begnami M, Quezado M, et al. Successful granulocyte-colony stimulating factor treatment of Crohn's disease is associated with the appearance of circulating interleukin-10-producing T cells and increased lamina propria plasmacytoid dendritic cells. Clin Exp Immunol 2009;155(3):447-56.

[69] Saba S, Soong G, Greenberg S, Prince A. Bacterial stimulation of epithelial G-CSF and GM-CSF expression promotes PMN survival in CF airways. Am J Respir Cell Mol Biol 2002;27(5):561-7.

[70] Mendes V, Galvao I, Vieira AT. Mechanisms by Which the Gut Microbiota Influences Cytokine Production and Modulates Host Inflammatory Responses. J Interferon Cytokine Res 2019;39(7):393-409.

[71] Wang Y, Kim R, Hwang SJ, Dutton J, Sims CE, Allbritton NL. Analysis of Interleukin 8 Secretion by a Stem-Cell-Derived Human-Intestinal-Epithelial-Monolayer Platform. Anal Chem 2018;90(19):11523-30.

[72] Song DH, Lee JO. Sensing of microbial molecular patterns by Toll-like receptors. Immunol Rev 2012;250(1):216-29.

[73] Walter MJ, Kajiwara N, Karanja P, Castro M, Holtzman MJ. Interleukin 12 p40 production by barrier epithelial cells during airway inflammation. J Exp Med 2001;193(3):339-51.

[74] Peluso I, Pallone F, Monteleone G. Interleukin-12 and Th1 immune response in Crohn's disease: pathogenetic relevance and therapeutic implication. World J Gastroenterol 2006;12(35):5606-10.

[75] Cane G, Moal VL, Pages G, Servin AL, Hofman P, Vouret-Craviari V. Up-regulation of intestinal vascular endothelial growth factor by Afa/Dr diffusely adhering Escherichia coli. PLoS One 2007;2(12):e1359.

[76] Schlieve CR, Mojica SG, Holoyda KA, Hou X, Fowler KL, Grikscheit TC. Vascular Endothelial Growth Factor (VEGF) Bioavailability Regulates Angiogenesis and Intestinal Stem and Progenitor Cell Proliferation during Postnatal Small Intestinal Development. PLoS One 2016;11(3):e0151396.

[77] Levast B, Li Z, Madrenas J. The role of IL-10 in microbiome-associated immune modulation and disease tolerance. Cytokine 2015;75(2):291-301.

[78] Mishima Y, Oka A, Liu B, Herzog JW, Eun CS, Fan TJ, et al. Microbiota maintain colonic homeostasis by activating TLR2/MyD88/PI3K signaling in IL-10-producing regulatory B cells. J Clin Invest 2019;129(9):3702-16.

[79] Veremeyko T, Siddiqui S, Sotnikov I, Yung A, Ponomarev ED. IL-4/IL-13-dependent and independent expression of miR-124 and its contribution to M2 phenotype of monocytic cells in normal conditions and during allergic inflammation. PLoS One 2013;8(12):e81774.

[80] Ma YL, Huang FJ, Cong L, Gong WC, Bai HM, Li J, et al. IL-4-Producing Dendritic Cells Induced during Schistosoma japonica Infection Promote Th2 Cells via IL-4-Dependent Pathway. J Immunol 2015;195(8):3769-80.

[81] Bahrami B, Macfarlane S, Macfarlane GT. Induction of cytokine formation by human intestinal bacteria in gut epithelial cell lines. J Appl Microbiol 2011;110(1):353-63.

[82] Lugering N, Kucharzik T, Kraft M, Winde G, Sorg C, Stoll R, et al. Interleukin (IL)-13 and IL-4 are potent inhibitors of IL-8 secretion by human intestinal epithelial cells. Dig Dis Sci 1999;44(3):649-55.

[83] Thorn M, Raab Y, Larsson A, Gerdin B, Hallgren R. Intestinal mucosal secretion of basic fibroblast growth factor in patients with ulcerative colitis. Scand J Gastroenterol 2000;35(4):408-12.

[84] Jung HC, Eckmann L, Yang SK, Panja A, Fierer J, Morzycka-Wroblewska E, et al. A distinct array of proinflammatory cytokines is expressed in human colon epithelial cells in response to bacterial invasion. J Clin Invest 1995;95(1):55-65.

[85] Rettedal E, Gumpert H, Sommer MOA. Cultivation-based multiplex phenotyping of human gut microbiota allows targeted recovery of previously uncultured bacteria. Nature Communications 2014;5.

[86] Kuczynski J, Stombaugh J, Walters WA, González A, Caporaso JG, Knight R. Using QIIME to analyze 16S rRNA gene sequences from microbial communities. Current protocols in bioinformatics 2011;Chapter 10:Unit 10.7.

[87] McDonald D, Price MN, Goodrich J, Nawrocki EP, DeSantis TZ, Probst A, et al. An improved Greengenes taxonomy with explicit ranks for ecological and evolutionary analyses of bacteria and archaea. ISME J 2012;6(3):610-8.

[88] Bolyen E, Rideout JR, Dillon MR, Bokulich NA, Abnet CC, Al-Ghalith GA, et al. Reproducible, interactive, scalable and extensible microbiome data science using QIIME 2. Nat Biotechnol 2019;37(8):852-7.

[89] Langille MG, Zaneveld J, Caporaso JG, McDonald D, Knights D, Reyes JA, et al. Predictive functional profiling of microbial communities using 16S rRNA marker gene sequences. Nat Biotechnol 2013;31(9):814-21.

[90] Hall RL, Miller RJ, Peatfield AC, Richardson PS, Williams I, Lampert I. A colorimetric assay for mucous glycoproteins using Alcian Blue proceedings. Biochemical Society transactions 1980;8(1):72.

Figures

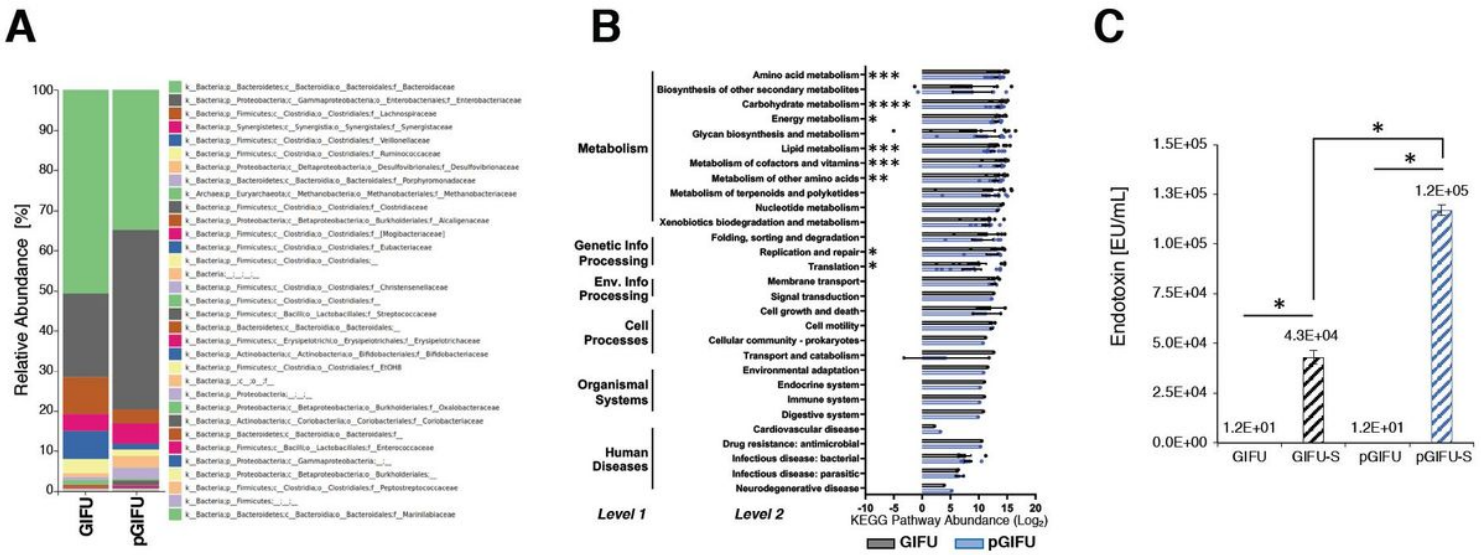

Figure 1

(A) Relative abundance at family level of taxonomy of GIFU and pGIFU microbiota. (B) Relative abundance of genetic functions grouped into KEGG pathway levels (BRITE hierarchy) and expressed as the sum of the predicted functional abundance (Level 3) contributed by each OTU multiplied by the

abundance of each OTU. Histogram bars indicate mean of Log2(Level 3 pathway abundance) +/- SEM, * p < 0.05; ** p < 0.01, *** p < 0.001, and **** p < 0.0001. (C) Endotoxin levels of different test media. * p < 0.05.

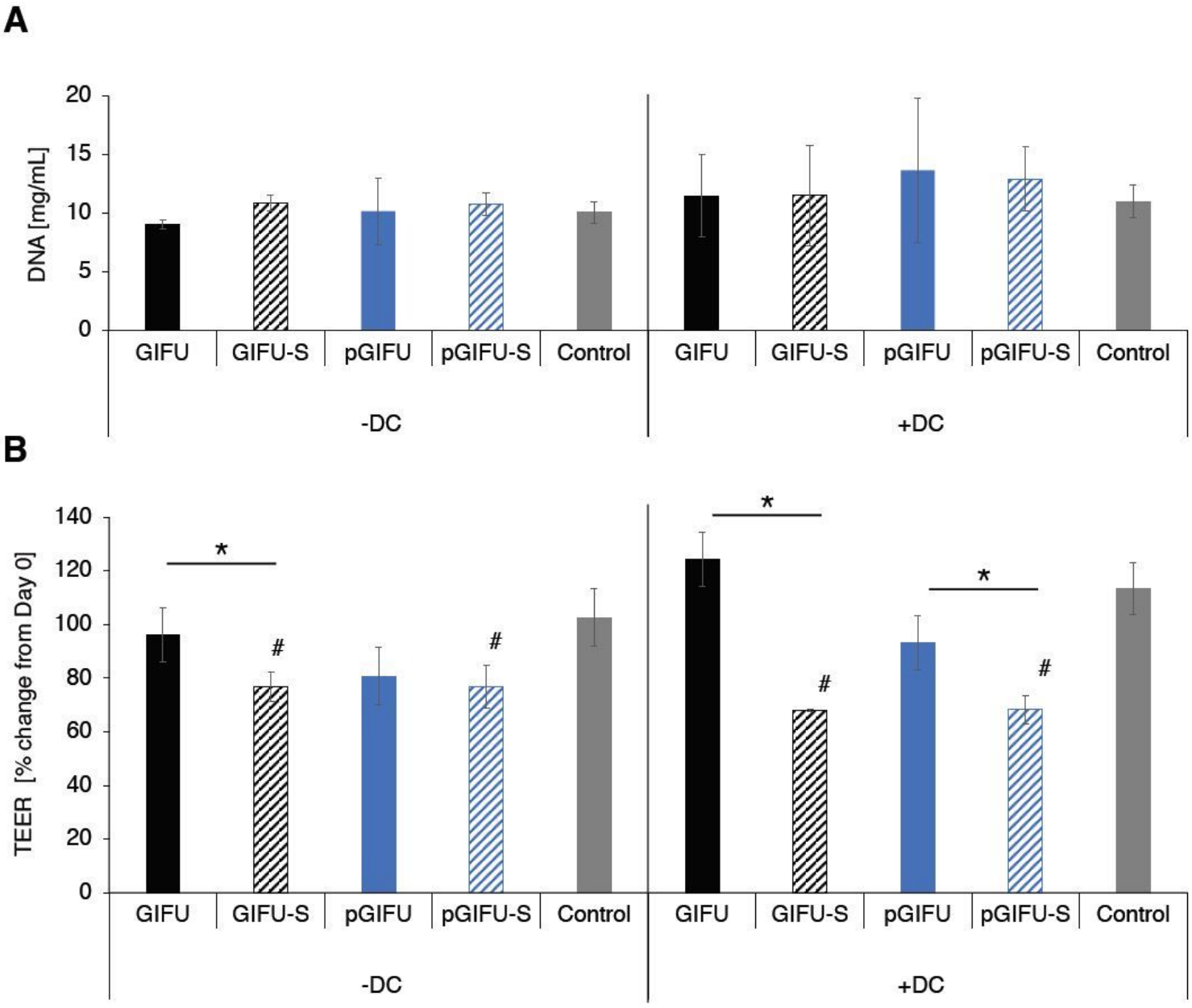

Figure 2

(A) DNA concentration of Caco2/HT29-MTX monolayers with and without dendritic cells (-/+ DC) exposed to different test media. (B) Trans-epithelial electrical resistance (TEER) indicating intestinal barrier function after 24 hr exposure of monolayers to test media. * p < 0.05 comparing spent vs. fresh, and # p < 0.05 compared to control serum-free intestinal cell culture media. All measurements were collected from an N=3 and results reported as an average ± standard deviation.

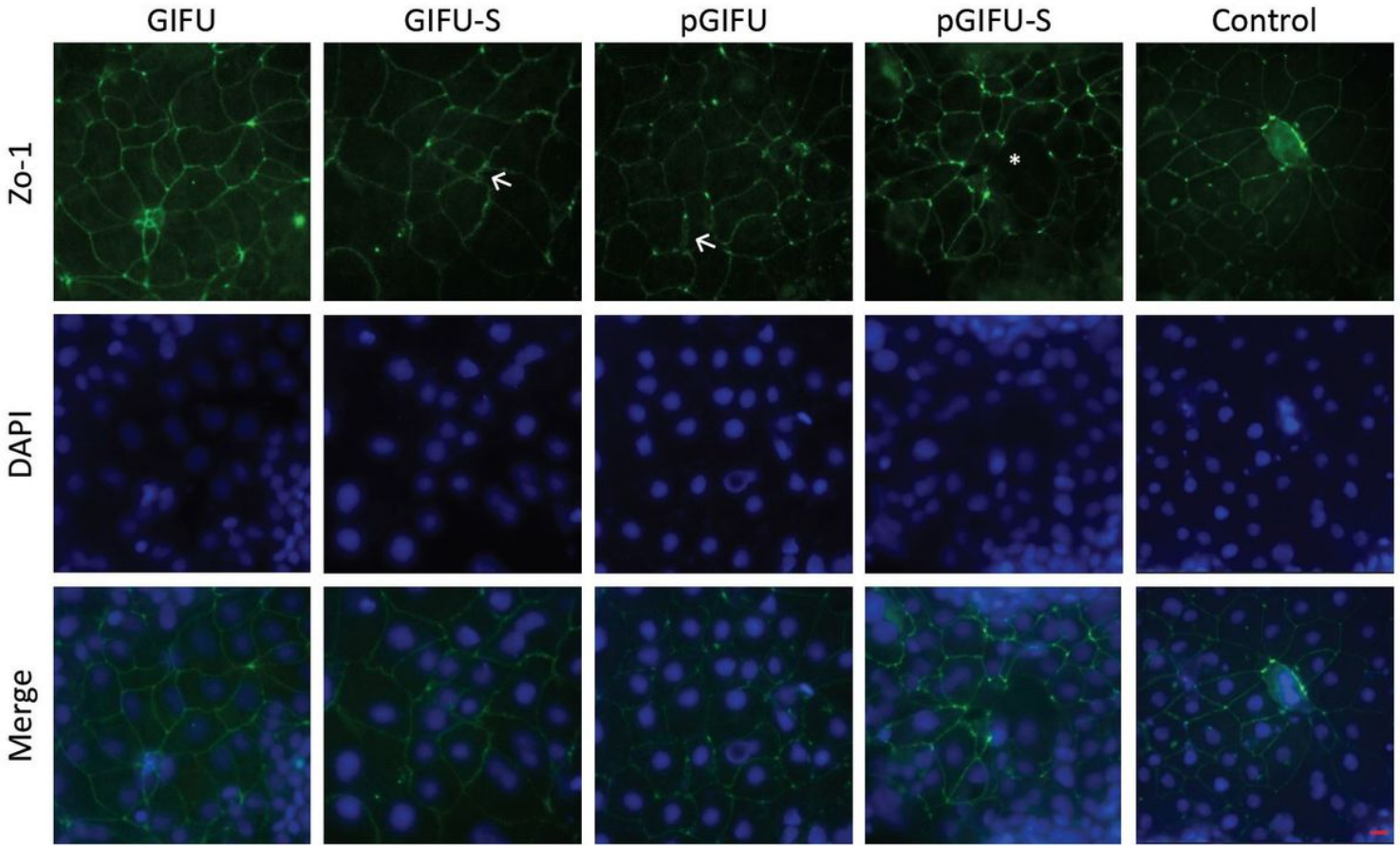

Figure 3

Co-cultures with dendritic cells stained for tight junction (ZO-1, green) and DNA (DAPI, blue). (←) indicates areas of zig-zag ZO-1 staining pattern and (*) denotes low ZO-1 staining. Scale bar: 20 μm.

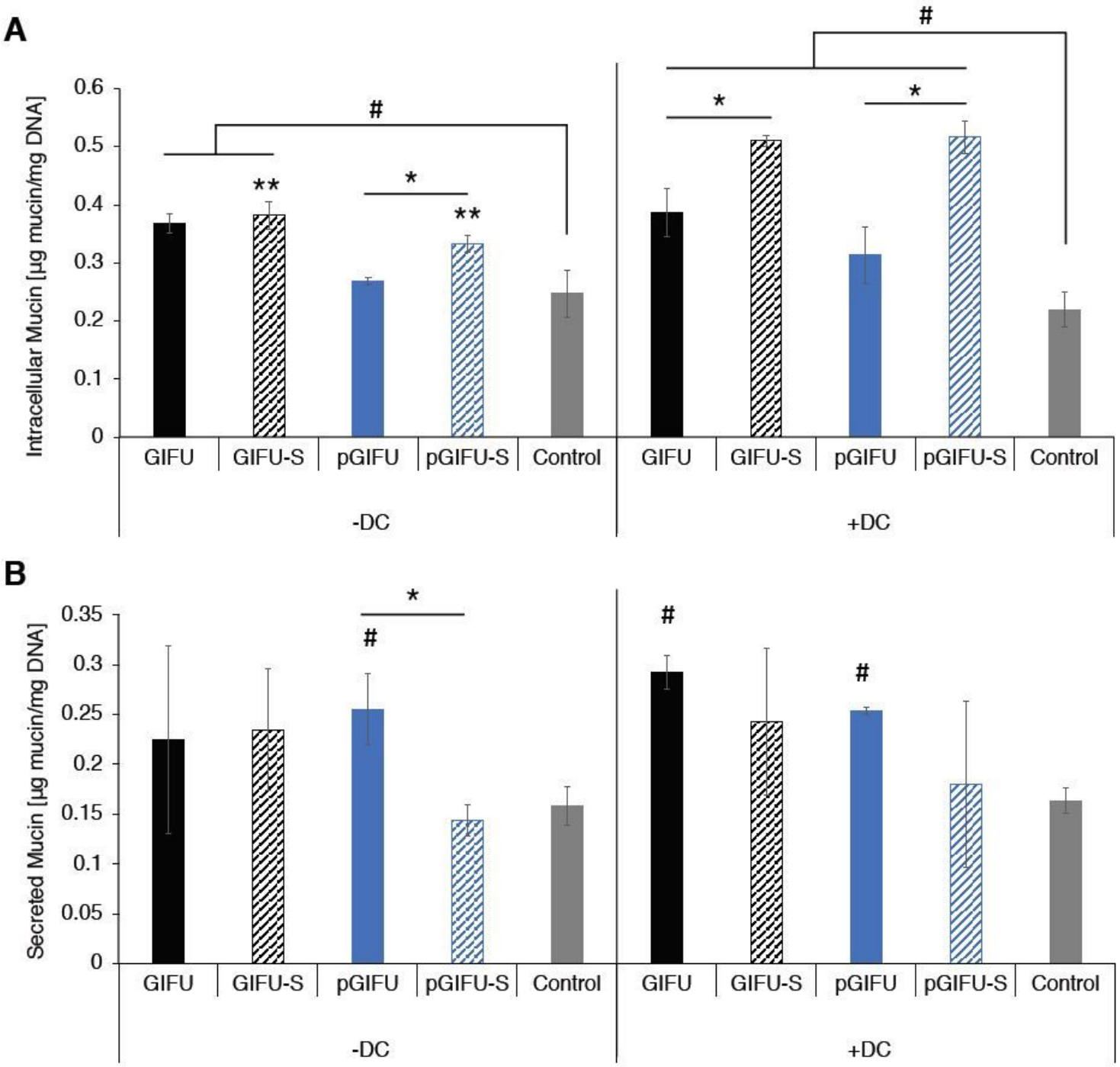

Figure 4

(A) Secreted and (B) intracellular mucin concentration from Caco2/HT29-MTX monolayers with and without dendritic cells (-/+ DC) after exposure to test media. * $p < 0.05$ comparing spent vs. fresh, ** $p < 0.05$ comparing -DC and +DC, and # $p < 0.05$ compared to control. All measurements were collected from an N=3 and results reported as an average ± standard deviation.

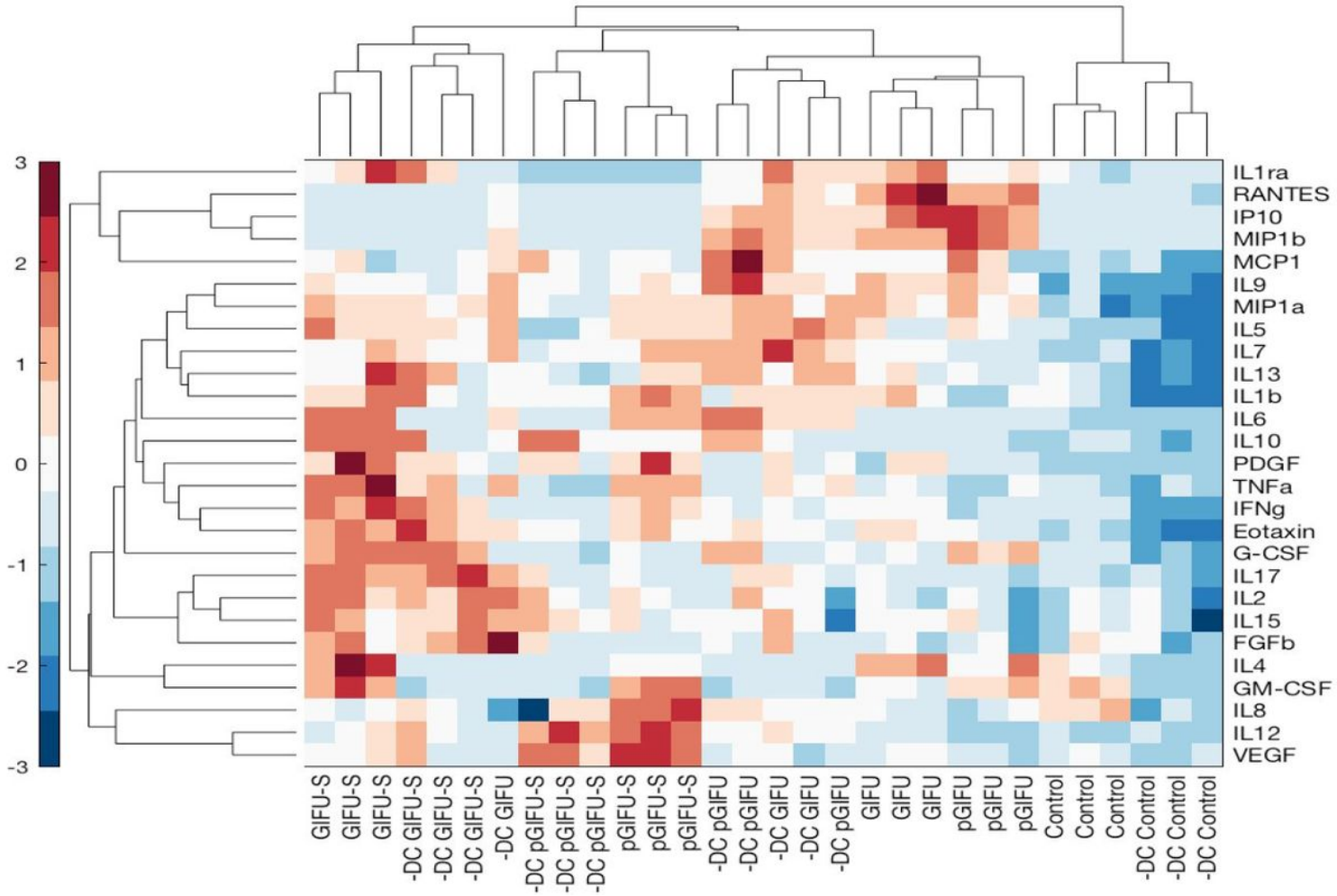

Figure 5

Hierarchical clustering of cytokine z-scores in different experimental groups. The cytokine levels are normalized to DNA concentration, mean-centered, and divided by standard deviation to generate z scores. Color bar indicates the relative cytokine amount, where red and blue correspond to high and low concentrations, respectively.

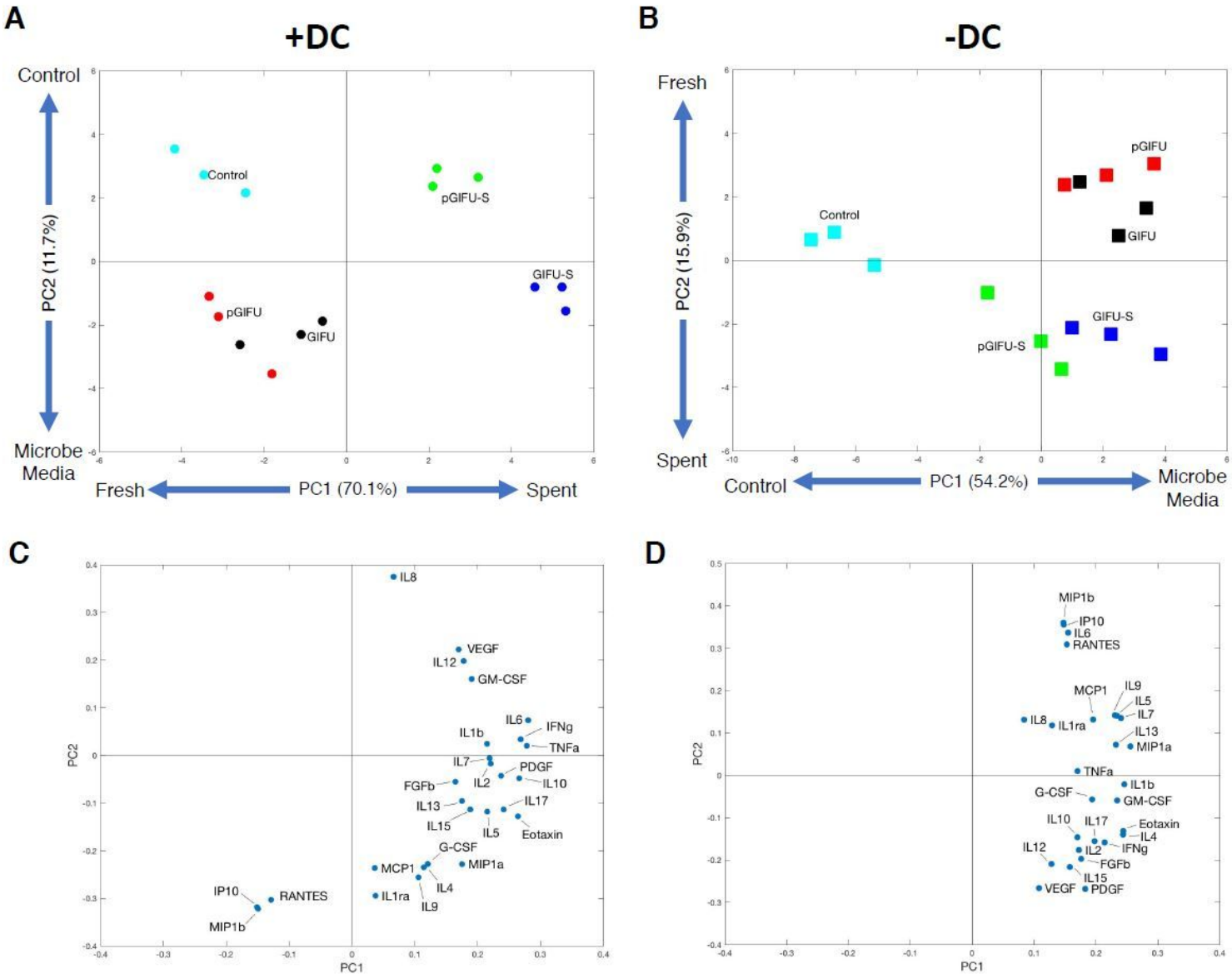

Figure 6

(A, B) Scores and (C, D) Loadings plots for a two-component PCA model on cultures (A, C) +DC and (B, D) - DC.

Supplementary Files

This is a list of supplementary files associated with this preprint. Click to download.

- SupplementAupdated01Sept20.xlsx
- SupplFig206Sept20.pdf
- SupplFig1.pdf